RSC Advances

ROYAL SOCIETY OF CHEMISTRY

www.rsc.org/advances

Adsorption and Photocatalytic Degradation Behaviors of Rhodamine Dyes on Surface-Fluorination TiO_2 under Visible Irradiation

Jing Guo,[a] Shaojun Yuan,[a] Wei Jiang,[a] Hairong Yue,[a] Zhe Cui, [b]Bin Liang[a,*]

[a] Multi-phase Mass Transfer & Reaction Engineering Lab,
College of Chemical Engineering,
Sichuan University, Chengdu 610065, China
[b] College of Material Science and Engineering,
Zhengzhou University, Zhengzhou, 450000, China

*To whom all correspondence should be addressed
Tel: +86-28-85460556, Fax: +86-28-85460556
E-mail: liangbin@scu.edu.cn

Abstract

Surface-fluorination TiO_2 (F-TiO_2) particles was synthesized by a simple fluorosilanization method to serve as a visible-light photocatalyst for rapid degradation of Rhodamine B (RhB) dyes. The fluroalkylsilane (FAS-17) was covalently immobilized on the TiO_2 particles via robust Si-O bonds. The changes in surface properties of the F-TiO_2 particles were characterized by *X*-ray photoelectron spectroscopy (XPS), Fourier transform infrared spectroscopy (FTIR), *X*-ray diffraction (XRD), scanning electron microscope (SEM) and zeta potential measurements. The optical property of the F-TiO_2 particles was determined by UV-visible spectroscopy. Upon the fluorination modification, the zeta potential of TiO_2 particles switched from positive to negative values, whilst the optical property of bulk TiO_2 particles remained almost unchanged. Photodegradation experimental results demonstrated that zwitterionic RhB dyes was more favorable to adsorb on the F-TiO_2 rather than on the Ti (IV) sites of the pristine TiO_2, and that the photodegradation reaction of RhB on the F-TiO_2 proceed much faster than that on the pristine TiO_2. However, the adsorption and photodegradation rate of anionic methyl orange (MO) dyes did not show obvious change on the F-TiO_2. These results suggested that the molecular structure of dyes played a key role in visible-light photodegradation reaction on the F-TiO_2 particles. Positive-charged diethylamine groups of RhB molecular structures was postulated to promote the adsorption of RhB dyes on the surface of F-TiO_2 particles, thus leading to easy electron injection and induction of rapid photodegradation under visible-light illumination.

Keywords: TiO_2, Surface Fluorination, Visible-light Photocatalysts, Photodegradation, Dyes

1. Introduction

Industrial development is pervasively connected with a copious amount of various toxic pollutants, which are hazardous to the environments, human health, and difficult to degrade by natural means. Conventional physicochemical and biological treatment methods, such as coagulation, adsorption, filtration, and anaerobic granular sludge, have been the main-stream techniques for the purification of organic compounds-contaminated water over past decades. However, these approaches are less effective to cleanse the anthropogenic organic pollutants at very low concentrations.[1] Photocatalysis, as an environmentally-benign approach, has therefore been attractive to treat persistent low-concentration organic pollutants in recent years.[2]

TiO_2 is the most extensively-studied photocatalysts in the decontamination of organic pollutants.[3] Under light illumination beyond its band-gap limits, TiO_2 shows strong oxidation ability to oxidize almost all organic compounds into CO_2. However, one obstacle toward its practical application is that TiO_2 can only be activated to induce photocatalytic reaction, by ultraviolet (UV) light, which accounts for only about 4% of the incoming sunlight. In view of practical applications, it is difficult to find an alternative photocatalyst as versatile, stable, abundant, environmentally-benign and economical as TiO_2. Consequently, modification of TiO_2 particles has been usually performed to achieve visible-light photosensitivity for effective photodegradation of organic pollutants under solar irradiation.

Various strategies have been proposed to modify TiO_2-based catalysts for enhanced visible light performance.[4-7] The doping (or incorporation) of metallic nano-materials, such as Cu_2O, WO_3, Ag and Au, into TiO_2 lattice has been found effective to improve the photocatalytic activities of TiO_2 in the visible light region. TiO_2 doped with nonmetallic elements, such as N,[8] S,[9] C,[10] I,[11] Br[12] and Cl,[13] has also been proven to shift the optical absorption edge of TiO_2 toward lower energy. A facile method to synthesize heterogeneous crystalline TiO_2–halloysite nanotubes

with anatase/rutile mixed phase has been descrived recently. The as-synthesized catalyst was found to have higher photocatalytic degradation of rhodamine B (RhB) and gentian violet than the commercial titania P25.[14] TiO_2 hybridized with a conducting polymer such as polyaniline has also verified to enhance photocatalytic activity towards the decomposition of organic molecules when irradiated with visible light.[15] In a whole, the above doping approaches are aimed to alter the absorption band of bulk TiO_2 to visible region by either narrowing the band-gap of TiO_2 or introducing new absorption band. Most of them focus mainly on the improvement of the visible response of TiO_2 by changing band-gap and other thermodynamic properties, but the kinetic properties are seldom investigated. Heterogeneous photocatalytic reactions primarily take place on the TiO_2 surface, hence surface features of TiO_2 are critical to the photocatalytic efficiencies. However, surface modification of TiO_2 does not shift the band energy to the visible light regions, it usually alters the adsorption, surface acidity, surface charge, and surface functional groups of TiO_2 surfaces, thus leading the change of the photocatalytic activities and mechanisms.[16]

In recent years, photosensitization of dyes has been reported to be one of the most effective ways to extend the photoresponse of TiO_2 into the visible region.[17, 18] In such a system, the dye pollutants rather than the TiO_2 photocatalyst are subject to the visible light excitation. The dye molecules are excited by visible-light illumination to transfer electrons into the conduction band of TiO_2, thus resulting in the formation of cationic radicals of the dyes. The injected electrons then react with O_2 molecules adsorbed on the surface of TiO_2 to generate a series of active oxygen radicals, such as $O_2^{-\cdot}$, $HO\cdot$, and H_2O_2 species. The subsequent radical chain reactions lead to the degradation and mineralization of the dye pollutants.[19-21] Because the photosensitization of dyes under visible irradiation can be initiated by the interfacial electron injection from the excited dye molecule into the TiO_2 catalyst, more adsorption of dyes may enhance interfacial interactions between dyes and TiO_2 to improve the photosensitization ability. Zhao et al reported that rapid and more adsorption of dyes on the TiO_2 particles caused the substantial enhancement of the extrinsic adsorption bands, thus leading to the increase in the degradation rate.[22]

Among various strategies to modify TiO_2 pariticles, surface fluorination of TiO_2 has been widely investigated.[23, 24] The fluorine-doped or surface fluorinated TiO_2 particles exhibited the enhanced photocatalytic activity under the UV and visible light illumination. Wang et al reported that surface fluorination not only changed the adsorption modes of dyes on the fluorinated TiO_2, but also caused the dramatic change in the photocatalytic degradation kinetics and mechanisms of the adsorbed dyes.[21] Surface fluorinatied TiO_2 has been also reported to be more effective than pure TiO_2 for the photocatalytic oxidation of acid orange 7 and phenol,[23] as they could enhance both photocatalytic reactions and photoelectrochemical behaviors. In the previous studies, surface fluorinations were also achieved by adding NaF into the dispersions under acidic conditions (pH 3-4), thus resulting in the replacement of surface hydroxyl groups by fluoride anion (F^-),[23, 25] or the dissolution of anatase TiO_2 to etch the surface of rutile TiO_2 by HF.[21, 26] The NaF-modified TiO_2 was found to significantly enhance the photocatalytic activities to dyes under UV light irradiation, but its photocatalytic ability was lower than the pristine TiO_2 under visible light irradiation.[23] However, to the best of our knowledge, few researches have been documented to surface fluorination of TiO_2 particles by a simple fluorosilanization process.

Herein, the aim of this work is to fluorinate TiO_2 particles by fluorosilanization for enhanced photocatalytic degradation of dyes under visible light illumination. The fluorosilane FAS-17 was chosen due to its low surface energy, abundant fluorine atoms and big electronegativity. The surface-fluorinated TiO_2 (F-TiO_2) particles were characterized by *X*-ray photoelectron spectroscopy (XPS), *X*-ray diffraction (XRD), Fourier transform infrared spectroscopy (FTIR), scanning electron microscope (SEM) and zeta potential measurements. The change in optical properties of the F-TiO_2 surface was determined by UV-visible spectroscopy. The adsorption of a zwitterionic RhB dye and an anionic MO dye on the F-TiO_2 surface were investigated, and the photodegradation behaviors of these two dyes were determined under visible light illumination. The postulated degradation mechanism of the RhB dye on the F-TiO_2 particles was proposed to interpret the photodegradation behaviors of dyes under visible light illumination.

2. Experimental Section

2.1 Materials. Powder anatase TiO_2 was kindly provided by Taihai Co. (Panzhihua City, China). The chemicals, such as rhodamine B (RhB), and Methyl orange (MO),rhodamine 101 inner salt(Rh 101 inner), rhodamine 6G (Rh 6G) and solvents, such as ethanol, were obtained from Aladdin Reagent Co. (Shanghai, China) and were used as received without further purifications. 1H, 1H, 2H, 2H-Perfluorodecyltriethoxysilane (FAS-17) was purchased from Sicong Chemicals Co. (Xiamen, China). The deionized water used in the following experiments was purified using an Ultrapure reverse osmosis system (Ultrapure Technol. Co., Chengdu, China), and were used throughout the study. The molecular structures of RhB, Rh 101 inner, Rh 6G, and MO were schematically shown in Electric Supporting Information (ESI, Fig. S1).

2.2 Preparation of Surface-fluorinated TiO_2 Particles. The surface fluorination of TiO_2 particles with FAS-17 was performed using a typical procedure similar to those described previously.[27] A 0.3 ml aliquot of FAS-17 was firstly hydrolyzed in a 5 ml ethanol solution at ambient temperature under continuous stirring for 2 h. A 0.7 g aliquot of TiO_2 particles was ultrasonically dispersed in a 150 ml round flask containing 55 ml of ethanol for 30 min. Subsequently, the FAS-17 mixture was added dropwise into the round flask under continuous stirring. The fluorosilaniation of TiO_2 particles was allowed to proceed at 70 ℃ for 5 h with a reflux condenser. At the end of reaction, the surface-fluorinated TiO_2 (defined as F-TiO_2) particles were harvested by centrifugation at 6000 rpm and ultrasonically washed three times with copious amount of ethanol to remove the physically-adsorbed FAS-17, if any. The as-synthesized F-TiO_2 particles were finally dried in a vacuum oven at 90 ℃ overnight.

2.3 Surface Characterization. The crystalline structure of TiO_2 particles before and after surface fluorination was characterized by X-ray powder diffraction (XRD) (DX-2700, Dandong, China). The voltage and anode current were 40 kV and 30 mA, respectively. The monochromatic Cu Kα (1.54056 Å) and scanning mode with interval of 0.03 °and set time of 0.05 s were used to collect

the XRD pattern of TiO_2 particles. The change in surface morphology of the F-TiO_2 particles was characterized by a scanning electron microscope (SEM) (S-4800, Hitachi, Japan). The particle size distribution and zeta potential of the TiO_2 particles suspensions (0.1 g/L) were determined respectively, by dynamic laser scanning Nanoparticle and Zeta potential analyzer (ZEN3690, Malvern, UK), and the pH was adjusted between pH 2.5 and 11.0 using a 1 $mol \cdot L^{-1}$ NaOH and HCl solutions. The optical properties of the pristine TiO_2 and F-TiO_2 particles were characterized by a UV–Visible spectrophotometer with an integrating sphere (UV2100, Shimadzu, Japan). The surface composition of the F-TiO_2 was determined by X-ray photoelectron spectroscopy (XPS) (XSAM800, Kratos, UK) with monochromatized Al Kα radiation at constant dwell time of 100 ms and pass energy of 40 eV. The pressure in the analysis chamber was maintained at 10^{-7} to 10^{-9} Torr during each measurement. To compensate the surface charging effect, all the core-level spectra were referred to the C 1s hydrocarbon peak with binding energy (BE) at 284.6 eV. The photoluminescence spectra (PL) were recorded via a fluorescence spectrometer (F-7000, Hitachi, Japan).

The FTIR spectra of the RhB-adsorbed pristine TiO_2 and F-TiO_2 particles were obtained on a Fourier transform infrared spectrometer (Spectrum II L1600300, PerkinElmer) in the transmission mode. Prior to the measurement, the RhB adsorption process was as follows: the pristine TiO_2 and F-TiO_2 particles were dispersed separately in 16 mg/L solution of RhB with highly-speed stirring, and then allowed to adsorb overnight to reach the adsorption equilibrium. The RhB-adsorbed particles were subsequently harvested by centrifugation, and then dried in air at 35 ℃. All the operations were carried out in dark to prevent photodegradation of the adsorbed dyes. The TiO_2 particles dispersed in deionized water under the same conditions were used as the control for FTIR measurement.

2.4 Adsorption and Visible Light Photocatalysis Activities of Modified F-TiO_2 Particles. The photocatalytic degradation of RhB and MO was investigated to determine the photocatalytic

activities of F-TiO_2 particles under visible light illumination. A photoreactor equipped with a 1000 W xenon lamp was used to perform the photocatalysis experiments (Institute of Electric Light Source, Kaifeng, China). Typically, the xenon lamp was positioned inside a cylindrical Pyrex vessel and surrounded by a circulating water Pyrex jacket, which served to cool the lamp for stable reaction temperature. A cutoff filter was placed outside the Pyrex jacket to secure visible-light irradiation only.

To eliminate the interference caused by adsorption on the photodegradation behaviors of dyes on the pristine TiO_2 and F-TiO_2 particles, the adsorption profiles of zwitterionic RhB and anionic MO dyes were determined prior to the photocatalytic experiments. Typically, a 100 mg aliquot of particles was well dispersed in 10 mL of 16 mg/L dye aqueous solution by highly-speed stirring, and the adsorption was allowed to proceed for a predetermined time at ambient temperature. All the operations were performed in the dark to prevent the photocatalytic reactions. The dye concentration after adsorption was determined by a UV-visible spectrophotometer.

In the photocatalytic experiments, the TiO_2 suspension was prepared by adding 100 mg of TiO_2 particles to 10 mL of 16 mg/L dye (RhB or MO) aqueous solution, or alternatively adding 150 mg of TiO_2 particles to 30 ml of 10 mg/L dye (RhB, Rh 6G, or Rh 101 inner). Prior to visible light irradiation, the suspension was stirred in the dark for 1 h to reach the adsorption/desorption equilibrium on the TiO_2 particle surfaces under ambient air-equilibrated conditions. During the light irradiation process, the suspension was allowed to proceed under vigorous stirring for a predetermined time. At the end of photocatalytic reaction, the suspension was separated by centrifugation at 8000 rpm to remove the solid particles, and the supernatant was collected for further analyses. The concentration of the RhB, MO, Rh 6G and Rh 101 inner solution was determined by UV-visible spectrophotometry (TU-1810, Persee, China) at a wavelength of 553 nm, 465 nm, 526 nm and 575 nm, respectively.

3. Results and Discussion

3.1 Surface properties and structure of the F-TiO_2 Particles. The surface fluorination of TiO_2 particles was achieved by fluorosilanizing the TiO_2 particles with FAS-17, as schematically illustrated in Figure 1. The reaction involves the hydrolysis of FAS-17 to convert siloxane groups (Si-OC_2H_5) to silanol groups (-Si-OH) and the fluorosilanization of TiO_2 particles. TiO_2 particles have been widely recognized to possess abundant hydroxyl groups (-OH) on the surface.[28] The ligand-exchanging reaction between the surface hydroxyl groups (-OH) of TiO_2 and Si-OH of FAS-17 results in the formation of robust Si-O-Ti bonds.[29, 30] Meanwhile, the dehydration condensation reaction among the –Si-OH groups leads to the formation of polysiloxanes. The surface characteristics, crystalline structure and size distribution of the as-synthesized F-TiO_2 particles were characterized by SEM, XPS, XRD, UV-visible and zeta potential measurements. The detailed results are discussed as follows.

3.1.1 SEM imaging and size distribution. The change in surface morphologies of the TiO_2 particles before and after surface fluorination was characterized by SEM imaging. Figure 2 shows the respective SEM image and size distribution diagrams of the pristine TiO_2 and the F-TiO_2 particles. For pristine TiO_2 particles, a disordered porous structure is observed and the particle surface is smooth and angular (Fig. 2a). No obvious change in surface morphology can be observed on the F-TiO_2 particles, albeit that the surface of TiO_2 particles becomes rough due to the deposition of silane layers (Fig. 2c). Moreover, some particles appear to stick together due to the silanization treatment, thus leading to the increase in TiO_2 particle size. This result is further ascertained by the size distribution of the pristine TiO_2 and F-TiO_2 particles as shown in Figures 2b and 2d. The average diameter of pristine TiO_2 is 278.1 $\pm$3 nm, while the average diameter of F-TiO_2 increases to 318.1 $\pm$3 nm (Table 1) upon the surface fluorination. The noticeable increase in the average diameters of F-TiO_2 particles is caused by both the deposition of FAS-17 layer and the aggregation of some TiO_2 particles.

3.1.2 FTIR and XPS spectra. The changes in surface chemistry of the TiO_2 particles before and after surface fluorination were ascertained by the FTIR measurement. Figure S2 (Electric Supporting Information) shows the respective FTIR spectra of the pristine TiO_2 and F-TiO_2 particles. The peak centered at a wavenumber of 3400 cm^{-1} (ESI, Fig. S2a), attributable to the stretching vibrations of hydroxyl groups (-OH), confirms the presence of reactive -OH on the pristine TiO_2 surfaces. The broad peak, centered at a wavenumber of around 1632 cm^{-1} is associated with the molecularly-adsorbed water (H–O–H bending vibrations) (ESI, Fig. S2b).[31-33] The successful fluorination of TiO_2 surfaces can be deduced from the appearance of three additional bands with wavenumber at 1153, 1206, and 1247 cm^{-1}, attributable to the stretching vibration of C-F species (ESI, Fig. S2b). These C-F species are characteristic peaks of fluorosilane FAS-17.

The surface composition of the FAS-17-modified TiO_2 was also characterized by XPS. Figure 3 shows the wide scan, C 1s and F 1s core-level XPS spectra of the pristine TiO_2 and F-TiO_2 particles, respectively. In comparison with the wide scan XPS spectrum of the pristine TiO_2 surface (Fig. 3a), four additional photoelectron lines with binding energies (BEs) at 99, 151, 685 and 832 eV, attributable to Si 2p, Si 2s, F 1s and F KLL species,[34] respectively, are discernible in the wide scan spectrum of the F-TiO_2 particle surface (Fig. 3a), indicative of the successfully immobilization of FAS-17 layer onto the TiO_2 surface. The presence of FAS-17 layer on the TiO_2 surface can also be deduced from the curve-fitted C 1s core-level spectrum, which consists of six peak components with BEs at 283.1, 284.8, 285.6, 289.4, 291.4 and 293.8 eV, attributable to C-Si, C-H, C-CFx , CF -CFx, C-F_2 and C-F_3 species,[35] respectively (Fig. 3b), as well as the appearance of the F 1s core-level spectrum with BE at 689 eV (Inset of Fig. 3b). The fluorine peak components of C-CFx, CF -CFx, C-F_2 and C-F_3 species are characteristics of the FAS-17 molecules.[27] Thus, the surface fluorination of TiO_2 particles has been successfully synthesized by covalently immobilizing of FAS-17.

3.1.3 XRD patterns. The change in crystalline structure of the TiO_2 particles before and after surface fluorination was characterized by XRD (ESI, Fig. S3). Despite of the coverage of fluorosilane layers on the TiO_2 particle surfaces, no significant shift in peak position of TiO_2 phase is observed from the XRD pattern of the F-TiO_2. This result is consistent with the fact that the FAS-17 layers do not be embedded into the TiO_2 lattices during surface fluorination. The persistence of the crystalline structure of TiO_2 particles after fluorosilanization is in good agreement with the previous findings that the surface fluorination, unlike the fluorine doping of TiO_2, cause no significant alternation in crystalline structures of TiO_2 particles.[24, 36]

3.1.4 UV-visible spectra. The change in optical properties of the TiO_2 particles before and after modification was determined by UV-visible spectroscopy (ESI, Fig. S4). It is evident that no significant shift in the fundamental absorption edge of TiO_2 (about 3.31 eV) is caused by the surface fluorination modification. This result is in good agreement with the previous conclusions that the surface fluorination modification has no effect the optical absorption edge of TiO_2.[23] Particularly, even the F-doped TiO_2 particles cannot cause the alternation of the optical absorption edge of TiO_2 particles, as reported previously by Yamaki et al.[37]

3.1.5 Zeta potential. The surface charge of the TiO_2 particles before and after surface fluorination was characterized by zeta potential measurement, and the results are summarized in Table 1. The zeta potential of TiO_2 particles at different pH conditions was measured to determine the effect of pH values on the surface charge of TiO_2 particles. The change in zeta potential of the pristine TiO_2 and F-TiO_2 particles as a function of pH values is shown in ESI Figure S5. The zeta potentials of both pristine TiO_2 and F-TiO_2 particles show an evident decrease with the increase in pH values. The point of zero charge (pzc) of the pristine TiO_2 is estimated to be about pH 7.8, while the pzc value of the F-TiO_2 particles shifts to around pH 4.7. This result indicates that the surface charge of TiO_2 particles is substantially influenced by surface fluorination. As shown in Table 1, at pH 6.5, the zeta potential of TiO_2 particles undergoes a dramatic change from positive

to negative values after the surface fluorinated modification. The pristine anatase TiO_2 particles show a positively-charged surface with the averaged zeta potential value of 7.2 ±1 mV, while the F-TiO_2 particles have a negatively-charged surface with zeta potential values of -21.1 ± 2 mV. The opposite change in the surface charge of the F-TiO_2 particles is probably associated with the presence of abundant fluorine atoms of the FAS-17. It has been reported that fluorine can effectively lower the surface free energy due to its small atomic radius and being as the biggest electronegativity among atoms.[27]

3.2 Photocatalytic activities of the modified F-TiO_2 under visible light irradiation

3.2.1 Adsorption behaviors of dyes on the modified F-TiO_2 Particles. In general, the observed photocatalyitc activity of a photocatalyst is a combined effect of many factors, such as surface area, phase structure, crystallinity, surface hydroxyl density, and surface charge.[38, 39] Pre-adsorption is indispensable for dyes to be photodegraded on the TiO_2 particle surface, since rapid adsorption of dyes facilitates electron injection. To further elucidate the effect of surface fluorination on the dye adsorption, the adsorption behaviors of zwitterionic RhB and anionic MO dyes were investigated for the pristine TiO_2 and the F-TiO_2 particles under continuous stirring in the dark. Figure 4 shows the adsorption profiles of RhB and MO on the pristine TiO_2 and the F-TiO_2 particles as a function of adsorption time, respectively. The pristine TiO_2 shows no adsorption to both dyes in the dark, as the concentration of the RhB and MO solution remained almost unchanged. However, the F-TiO_2 particles show different adsorption behaviors to RhB and MO dyes. The pre-adsorption of RhB on the F-TiO_2 particles increase rapidly to about 60%, and reach adsorption equilibrium afterwards (Fig. 4b), while no pre-adsorption of MO on the F-TiO_2 particles is observed (Fig. 4b). This phenomenon is probably associated with the electrostatic interaction between the F-TiO_2 and zwitterionic RhB dyes. After fluorination, the TiO_2 particles become more electronegative, and possess the negative surface charge at pH 6.5. Therefore, the negatively-charged F-TiO_2 particle facilitates the adsorption of positively-charged diethylamine

group in the RhB molecules owing to electrostatic attraction, while it hinders the adsorption of anionic MO dye due to the electrostatic repulsion.

3.2.2 Photodegradation activities of dyes on the modified F-TiO_2 Particles. After the adsorption equilibrium of RhB with TiO_2 and F-TiO_2 had been achieved, the photocatalytic decomposition experiment was performed under irradiation with visible light to evaluate the photocatalytic ability of F-TiO_2 particles. Fig. 5 shows the photodegradation curves of RhB without and with the presence of TiO_2 particles before and after subtracting the adsorbed amount. The RhB dyes remain unchanged under visible light illustration in the absence of TiO_2 particles over 120 min (Fig. 5a), while the degradation ratio of the RhB dyes by the pristine TiO_2 particles is about 65% (Fig. 5b). On the other hand, the enhancement in photocatalytic degradation of RhB under the visible-light irradiation can be observed on the F-TiO_2 particles, since the photodegradation ratio of the RhB dyes by the F-TiO_2 particles reach as high as more than 99% after 120 min (Fig. 5b). Moreover, no degradation of the RhB dye solution containing FAS-17 is observed under the visible light illumination, indicative of no visible-light photocatalytic properties of the FAS-17 molecules. Similarly, no degradation of RhB dyes takes place in the dark in the presence of the F-TiO_2 particles. The above results are consistent with the fact that the visible-light photocatalytic activities are significantly enhanced by the F-TiO_2 particles.

To investigate the role of surface fluorination in affecting the photodegradation kinetics and mechanisms of dyes, the photodegradation of anionic MO dyes were also examined, and the photocatalytic degradation behaviors of the anionic MO dyes for the pristine TiO_2 and F-TiO_2 particles under visible-light irradiation are show in Figure 6. The MO dyes remains unchanged throughout under visible-light irradiation in the absence of TiO_2 particles. Particularly, the MO dyes also remain relatively stable in the presence of photocatalysts, since the photodegradation ratios of the MO dyes by the pristine TiO_2 and the F-TiO_2 are only about 8% and about 11%, respectively, after 120 min of visible-light irradiation. These results suggest that the surface fluorination of TiO_2 particles cannot improve the visible-light photocatalytic activity of the

anionic MO dyes. Taking together, the surface fluorination of TiO_2 particles can only lead to the selectively-enhanced photocatalytic activity to the zwitterionic RhB dyes rather than to the anionic MO dyes. This phenomenon is possibly ascribed to the enhanced pre-adsorption of RhB and the intrinsic sensitivity of RhB to visible light illumination for the F-TiO_2 particles. It has been reported that the adsorption behaviors of cationic dyes on the catalyst surface play an important role in improving their photocatalytic degradation rate.[22]

The pre-adsorption of the zwitterionic RhB dyes on the F-TiO_2 particles rapidly reaches as high as 60% prior to the visible light irradiation (Figs. 4 and 5a), while the anionic MO dyes show almost no pre-adsorption on the F-TiO_2 particles. As a consequence, the enhancement in visible-light photocatalytic degradation of the zwitterionic RhB dyes is probably ascribed to, the enhanced pre-adsorption and the intrinsic visible-light sensitivity of zwitterionic RhB dyes, as compared to the anionic MO dyes. To further confirm the effect of dye types and pre-adsorption of dyes on the photocatalytic ability, other two cationic dyes such as Rh 6G and Rh 101 inner were chosen to perform the photocatalytic degradation experiments by the pristine TiO_2 and F-TiO_2 particles. Similar to that of the zwitterionic RhB, the photocatalytic degradation ratios of the two cationic dyes by F-TiO_2 particles show a significant increase under visible light irradiation, and both reach higher than 95% (ESI, Fig. S6). These above results are in good agreement with the previous findings that the dye structure and their anchoring groups on the photocatalyst are key factors to determine the interfacial electron transfer and the degradation ratio of the dye.[19]

3.2.3 The degradation of adsorbed dyes characterized by FTIR analyses. As about 60% of the RhB is adsorbed on the F-TiO_2 particles, it is of great importance to verify the degradation of the RhB adsorbed on the F-TiO_2 surfaces. Despite that the pink-colored F-TiO_2 particles has been turned to white after light irradiation, the RhB-adsorbed F-TiO_2 were further characterized by FTIR and UV-visible spectra to ascertain the photodegradation of RhB dyes on the F-TiO_2

surface. Figure 7 shows the respective FTIR spectra of the F-TiO_2, RhB-adsorbed F-TiO_2 before and after visible-light illumination. By comparing the FTIR spectra of the three samples, the RhB dyes adsorbed on the F-TiO_2 surface are confirmed to be completely photo-degraded. As shown in Figure 7b, upon the adsorption of RhB dyes, two additional peaks with wavenumber at 1183 and 1340 cm^{-1}, attributable to the stretching vibrations of the C-O-C and the C-aryl groups, respectively.[40], appear on the FTIR spectra of the particles. The broad peak, centered at a wavenumber of around 1632 cm^{-1}, is attributed to the molecularly adsorbed water (H–O–H bending vibrations),[31] which is overlap with the C-N bond at a wavenumber of 1649 cm^{-1} (Fig. 7b).[21] However, these characteristic bands of RhB disappear in the FTIR spectrum of the RhB-adsorbed F-TiO_2 particles after visible-light irradiation (Fig. 7c). The FTIR results reveal that the RhB dyes adsorbed on the F-TiO_2 particle surfaces can be completely photodegraded under light irradiation.

3.2.4 Determination of the stability of the F-TiO_2 particles. To determine whether the release of fluorine ions can release from the F-TiO_2 particles during the photocatalytic processes, the stability of the fluorosilane layers was evaluated by the FTIR and UV-Vis spectra of the F-TiO_2 particles after visible-light radiation. As shown in Figure 7c, the characteristic bands with wavenumber at 1153, 1206, and 1247 cm^{-1}, attributable to the stretching vibration of C-F species, are still available, and the peak intensity also appears to remain unchanged as compared to the F-TiO_2 particles before visible-light illustration. These results suggest the good stability of the F-TiO_2 particles after light irradiation, and probably no fluorine release from the luorosilane layers. To further verify the good stability of F-TiO_2 particles, the optical properties of the F-TiO_2 particles after visible-light irradiation were also measured by the UV-Vis spectra (ESI, Fig. S7). No evident difference of the UV-Vis spectra can be distinguished from the visible-light irradiated F-TiO_2 particles as compared to the as-synthesized F-TiO_2 particles (ESI, Fig. S4). The fundamental absorption edge of F-TiO_2 after irradiation still remains at about 3.31 eV.

3.2.5 Recyclability of the F-TiO_2 particles To determine the recyclability of the F-TiO_2 particles, the used F-TiO_2 particles were harvested and recycled to the photocatalytic degradation of RhB under visible light irradiation. The photocatalytic degradation curves of the RhB in the presence of recycled TiO_2 and F-TiO_2 particles are shown in ESI Figure S8 (second cycle). Surprisingly, both the recycled TiO_2 and F-TiO_2 particles do not show any decrease in the photocatalytic ability to the RhB dyes, and even cause a slight increase in the photodegradation ratio of RhB dyes. The photocatalytic degradation ratio of the RhB dyes by the recycled TiO_2 particles is about 65%, while the photodegradation ratio of RhB by the recycled F-TiO_2 particles reaches as high as more than 90% after 80 min of visible-light irradiation (ESI, Fig. S8). These results confirm the good recyclability of the F-TiO_2 particles, and are consistent with the above FTIR data.

3.3 The postulated visible-light photocatalytic mechanisms of RhB dyes on the F-TiO_2 particles.

Under visible light irradiation, the degradation of zwitterionic RhB dyes is substantially enhanced in the presence of F-TiO_2 particles, while the degradation of anionic MO dyes shows no significant change. Therefore, it can be speculated that the enhanced photodegradation of RhB dyes is probably not caused by the intrinsic change of F-TiO_2 particles, but is more possibly associated with dye sensitization. As liquid–solid heterogeneous photocatalysis is a well-known interface-based process, the contact of dye molecules with the surface of catalyst is prerequisite to efficient electron transfer. The enhanced adsorption of dyes can also eliminate the outer diffusion control in surface reaction. Therefore, the enhanced adsorption of photosensitive dyes will partly contribute to the high photocatalytic activity of F-TiO_2. Take together, a postulated mechanism of the enhanced visible-light photocatalytic activity of RhB on the F-TiO_2 particles has been proposed, and is schematically illustrated in Figure 8. The positively-charged TiO_2 particle surfaces show the electrostatic repulsion to resist the adsorption of RhB dyes (Fig. 8a), while the negatively-charged F-TiO_2 surfaces show strong affinity to attract RhB dyes (Fig. 8b). According to the adsorption results (Fig. 4), the RhB dyes can rapidly adsorb onto the F-TiO_2 surface to reach

dynamic adsorption/desorption equilibrium. Thus, the pre-adsorption of RhB is an initial and important step to enhance visible-light photocatalytic degradation on the F-TiO_2 particle surfaces.

Figure 8c schematically illustrates the electron-transfer processes and subsequent excitation of RhB dye on the F-TiO_2 particle surfaces. As a matter of fact, the TiO_2 particles may be not excited as its absorption threshold is 385 nm under visible-light illumination, however, the adsorbed RhB on the TiO_2 surface can be excited at a wavelength longer than 470 nm to produce singlet and triplet states (denoted as RhB^*_{ads}). [22] The RhB^*_{ads} subsequently injects an electron into the conduction band (or to some surface states) of the TiO_2 particles to convert RhB to the radical cation $RhB^{\bullet+}$. In turn, the injected electron on the TiO_2 particles, TiO_2 (e^-), can react with adsorbed oxidants (usually O_2) to produce reactive oxygen radicals. The radical cation $RhB^{\bullet+}$ ultimately reacts with reactive oxygen radicals and/or molecular oxygen to yield intermediate products or other radical species, for which might lead to mineralization if secondary radical processes occurred.[41] As a consequence, the pre-adsorption of cationic RhB dyes and activation of the visible-light sensitive RhB dyes to inject electrons to TiO_2 particles are important steps to enhance the visible-light photodegradation activities of the TiO_2 particles.

To confirm the above postulated mechanism of the activation of pre-adsorbed RhB dyes to inject electron to TiO_2 particles, the photoluminescence (PL) signals was obtained on a fluorescence spectrometer. The PL signals of semiconductor materials result from the recombination of photo-induced charge carriers. Generally, the lower PL intensity, the lower the recombination rate of photo-induced electron–hole pairs, and the higher the photocatalytic activity of semiconductor photocatalysts.[42] Figure 9 shows the PL emission spectra of pure TiO_2, F-TiO_2 and F-TiO_2 adsorbed with RhB in the wavelength range 300–700 nm. The intensity of the PL spectrum of pure TiO_2 is much higher than that of the F-TiO_2 and F-TiO_2/RhB samples. The intensity of F-TiO_2/RhB is the lowest, it can be reasonably inferred that the enhanced adsorption of RhB dye should have a higher photocatalytic performance.

4. Conclusions

With the objective to enhance the visible-light photocatalytic degradation activities of TiO_2 to organic pollutants, a facile wet fluorosilanization approach was described to modify the anatase TiO_2 particles. Various surface characterization techniques, including XPS, XRD, zeta potential, SEM, FTIR and UV-Vis spectroscopy, were utilized to determine the surface characteristics change after the surface fluorination. The fluorination modification of TiO_2 surfaces caused no significant changes in the surface morphology, crystalline phase, and optical properties, but the dramatic alternation of surface charges from positive to negative values. As a result, both the adsorption modes and degradation of the dyes were greatly altered. Adsorption experimental results revealed that the F-TiO_2 particles had a high affinity to attract zwitterionic RhB dyes instead of anionic MO dyes due to the electrostatic interaction. The postulate mechanisms were proposed to interpret the electron transfer from the excited dyes to TiO_2 particles rather than the intrinsic electron and holes of TiO_2 particles.

Acknowledgements

The authors would like to acknowledge the financial assistance of key project of National Natural Science Foundation of China (NO. 21236004)

Supporting Information Available

Structures of all the dyes used (Fig. S1), FTIR Spectra (Fig. S2), X-ray diffraction patterns (Fig. S3), the forbidden bandwidth of the prestine TiO_2 and F-TiO_2 particles (Fig. S4), the zata potentials of the pristine TiO_2 and F-TiO_2 particles (Fig. S5), the photodegradation curves of Rh 6G and Rh 101 inner salt (Fig. S6), .the forbidden bandwidth of the F-TiO_2 after photodegradation (Fig. S7) and the photodegradation curves of the RhB dyes in the presence of recycled TiO_2 and F-TiO_2 particles (Fig. S8).

Reference

1. C. Chen, W. Ma and J. Zhao, *Chemical Society reviews*, 2010, **39**, 4206-4219.
2. K. Demeestere, J. Dewulf and H. Van Langenhove, *Critical reviews in environmental science and technology*, 2007, **37**, 489-538.
3. A. Fujishima, T. N. Rao and D. A. Tryk, *Journal of Photochemistry and Photobiology C: Photochemistry Reviews*, 2000, **1**, 1-21.
4. D. Chatterjee and A. Mahata, *Journal of Photochemistry and Photobiology A: Chemistry*, 2004, **165**, 19-23.
5. J. Choi, H. Park and M. R. Hoffmann, *The Journal of Physical Chemistry C*, 2009, **114**, 783-792.
6. J. Lin, R. Zong, M. Zhou and Y. Zhu, *Applied Catalysis B: Environmental*, 2009, **89**, 425-431.
7. B. Muktha, D. Mahanta, S. Patil and G. Madras, *Journal of Solid State Chemistry*, 2007, **180**, 2986-2989.
8. R. Nakamura, T. Tanaka and Y. Nakato, *The Journal of Physical Chemistry B*, 2004, **108**, 10617-10620.
9. T. Ohno, M. Akiyoshi, T. Umebayashi, K. Asai, T. Mitsui and M. Matsumura, *Applied Catalysis A: General*, 2004, **265**, 115-121.
10. S. U. Khan, M. Al-Shahry and W. B. Ingler, *science*, 2002, **297**, 2243-2245.
11. X. Hong, Z. Wang, W. Cai, F. Lu, J. Zhang, Y. Yang, N. Ma and Y. Liu, *Chemistry of Materials*, 2005, **17**, 1548-1552.
12. H. Irie, S. Washizuka, N. Yoshino and K. Hashimoto, *Chemical Communications*, 2003, 1298-1299.
13. S. Yamazaki, T. Tanimura, A. Yoshida and K. Hori, *The Journal of Physical Chemistry A*, 2004, **108**, 5183-5188.
14. C. Li, J. Wang, S. Feng, Z. Yang and S. Ding, *Journal of Materials Chemistry A*, 2013, **1**, 8045-8054.
15. C. Li, J. Wang, H. Guo and S. Ding, *Journal of colloid and interface science*, 2015, **458**, 1-13.
16. X. Quan, J. Niu, S. Chen, J. Chen, Y. Zhao and F. Yang, *Chemosphere*, 2003, **52**, 1749-1755.
17. Y. Cho, W. Choi, C.-H. Lee, T. Hyeon and H.-I. Lee, *Environmental science & technology*, 2001, **35**, 966-970.
18. T. Wu, T. Lin, J. Zhao, H. Hidaka and N. Serpone, *Environmental science & technology*, 1999, **33**, 1379-1387.
19. D. Zhao, C. Chen, Y. Wang, W. Ma, J. Zhao, T. Rajh and L. Zang, *Environmental science & technology*, 2007, **42**, 308-314.
20. P. Chowdhury, J. Moreira, H. Gomaa and A. K. Ray, *Industrial & Engineering Chemistry Research*, 2012, **51**, 4523-4532.
21. Q. Wang, C. Chen, D. Zhao, W. Ma and J. Zhao, *Langmuir*, 2008, **24**, 7338-7345.
22. J. Zhao, T. Wu, K. Wu, K. Oikawa, H. Hidaka and N. Serpone, *Environmental science & technology*, 1998, **32**, 2394-2400.
23. H. Park and W. Choi, *The Journal of Physical Chemistry B*, 2004, **108**, 4086-4093.
24. J. Tang, H. Quan and J. Ye, *Chemistry of materials*, 2007, **19**, 116-122.

25. J. Lee, W. Choi and J. Yoon, *Environmental science & technology*, 2005, **39**, 6800-6807.
26. R. Nakamura, T. Okamura, N. Ohashi, A. Imanishi and Y. Nakato, *Journal of the American Chemical Society*, 2005, **127**, 12975-12983.
27. C. Kang, H. Lu, S. Yuan, D. Hong, K. Yan and B. Liang, *Chemical Engineering Journal*, 2012, **203**, 1-8.
28. L. G. Bach, M. Islam, S. Y. Seo and K. T. Lim, *Journal of Applied Polymer Science*, 2013, **127**, 261-269.
29. A. Y. Fadeev and T. J. McCarthy, *Langmuir*, 2000, **16**, 7268-7274.
30. D. Schondelmaier, S. Cramm, R. Klingeler, J. Morenzin, C. Zilkens and W. Eberhardt, *Langmuir*, 2002, **18**, 6242-6245.
31. W.-C. Hung, S.-H. Fu, J.-J. Tseng, H. Chu and T.-H. Ko, *Chemosphere*, 2007, **66**, 2142-2151.
32. S. Sivakumar, P. K. Pillai, P. Mukundan and K. Warrier, *Materials letters*, 2002, **57**, 330-335.
33. S. Musić, M. Gotić, M. Ivanda, S. Popović, A. Turković, R. Trojko, A. Sekulić and K. Furić, *Materials Science and Engineering: B*, 1997, **47**, 33-40.
34. J. F. M. C.D. Wagner, J.E. Davis, W.M. Riggs,, *Handbook of X-ray Photoelectron Spectroscopy*, Perkin-Elmer Corp., Eden Prairie, MN, USA, 1992.
35. H. Liu, L. Pan, K. Shen, J. Lang, J. Shi, Q. Cui, H. Li and C. Liu, *Fertility and sterility*, 2009, **92**, 1150-1152.
36. D. Li, H. Haneda, N. K. Labhsetwar, S. Hishita and N. Ohashi, *Chemical Physics Letters*, 2005, **401**, 579-584.
37. T. Yamaki, T. Umebayashi, T. Sumita, S. Yamamoto, M. Maekawa, A. Kawasuso and H. Itoh, *Nuclear Instruments and Methods in Physics Research Section B: Beam Interactions with Materials and Atoms*, 2003, **206**, 254-258.
38. D. Li, H. Haneda, N. Ohashi, S. Hishita and Y. Yoshikawa, *Catalysis today*, 2004, **93**, 895-901.
39. D. Li, H. Haneda, N. K. Labhsetwar, S. Hishita and N. Ohashi, *Chemical Physics Letters*, 2005, **401**, 579-584.
40. N. Mchedlov-Petrossyan, S. Shapovalov, S. Egorova, V. Kleshchevnikova and E. A. Cordova, *Dyes and pigments*, 1995, **28**, 7-18.
41. R. W. Matthews, *Water Research*, 1991, **25**, 1169-1176.
42. J.-G. Yu, H.-G. Yu, B. Cheng, X.-J. Zhao, J. C. Yu and W.-K. Ho, *The Journal of Physical Chemistry B*, 2003, **107**, 13871-13879.

Figure Legends

Figure 1. Schematic illustration of the fluorosilanization process of FAS-17 onto the TiO_2 particles surfaces.

Figure 2. The SEM images and size distribution diagrams of (a, b) the pristine anatase TiO_2 and (c, d) the F-TiO_2 particles.

Figure 3. (a) Wide scan XPS spectra of the pristine TiO_2 (red line) and F-TiO_2 (black line) surfaces (b) the C 1s and F 1s core-level XPS spectra of the F-TiO_2 particle surface.

Figure 4. The adsorption profiles of (a) zwitterionic RhB and anionic MO on the pristine TiO_2 and (b) F-TiO_2 particles as a function of time in the dark. Adsorption conditions: initial dye concentration (C_0) of 16 mg L^{-1}, temperature: at room temperature.

Figure 5. (a) The photocatalytic degradation curves of RhB without and with the presence of TiO_2 particles as a function of time under visible light illumination, (b) the photodegradation curve of RhB after subtracting the adsorbed amount with the presence of TiO_2 and F-TiO_2 particles. Reaction conditions: (a) initial dye concentration (C_0) of 16 mg L^{-1}, catalyst dosage of 10 g L^{-1}, (b) initial dye concentration (C_0) of 10 mg L^{-1}, catalyst dosage of 5 g L^{-1}, light intensity: 1000 W xenon lights.

Figure 6. The photocatalytic degradation curves of MO with or without the presence of TiO_2 particles as a function of time under visible light illumination. Reaction conditions: initial dye concentration (C_0) of 16 mg L^{-1}, catalyst dosage of 10 g L^{-1}, light intensity: 1000 W xenon lights.

Figure 7. FTIR spectra of the (a) as-synthesized F-TiO_2, (b) F-TiO_2 adsorbed with RhB, and (c) F-TiO_2 after degradation of the adsorbed RhB.

Figure 8. Schematic illustration of (a, b) the adsorption model of the cationic RhB dyes on the pristine TiO_2 and F-TiO_2 particle surface, and (c) electron-transfer processes and subsequent excitation of RhB dye on the F-TiO_2 particle surfaces.

Figure 9. The PL spectrum of the pristine anatase TiO_2 (black line), the F-TiO_2 (red line) and the RhB-adsorbed F-TiO_2 (blue line). The adsorption experimental conditions: initial dye concentration (C_0) of 100 mg L^{-1}, catalyst dosage of 10 g L^{-1}.

Table 1. The average particle size and zeta potential of TiO_2 particles before and after surface fluorination

	Anatase	F-TiO_2
Zeta potential values (mv)[a]	7.2 ±1	-21.1 ±2
Particle sizes (nm)	278.1±3	318.1±3

[a]zeta potentials of TiO_2 particles were obtained at pH 6.5.

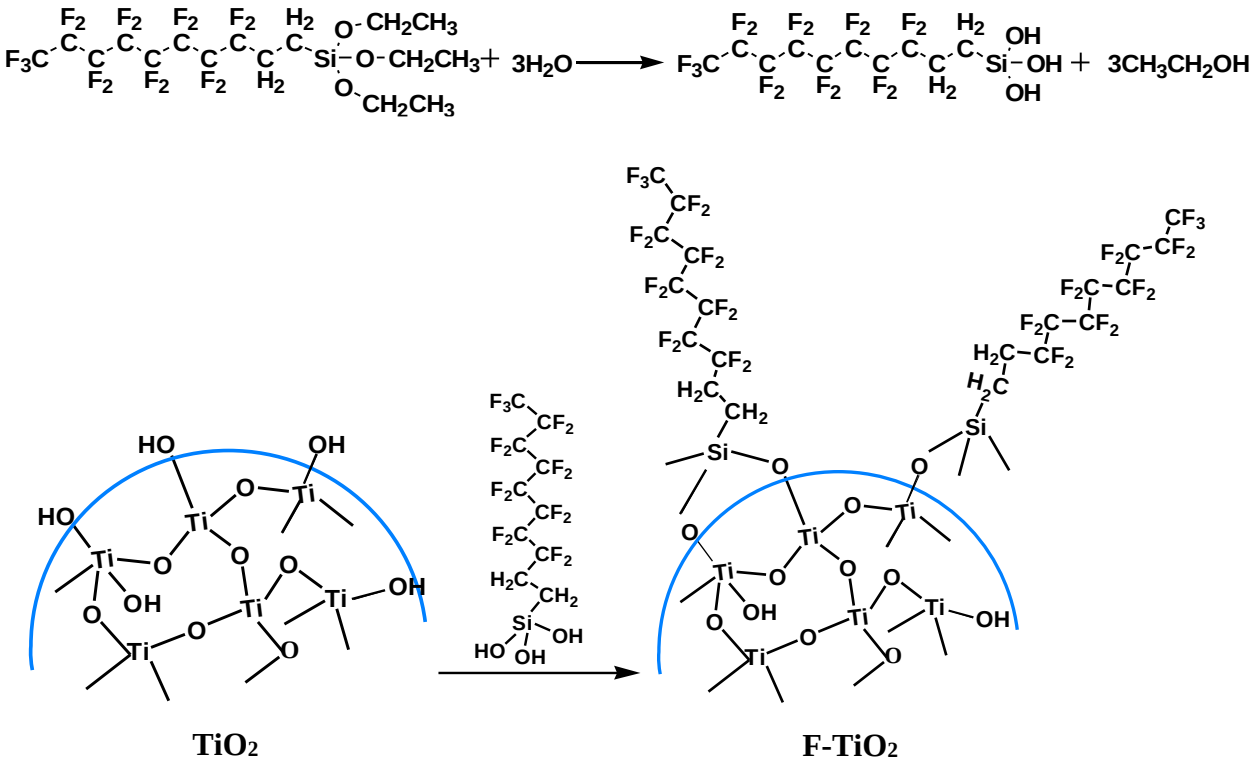

Figure 1

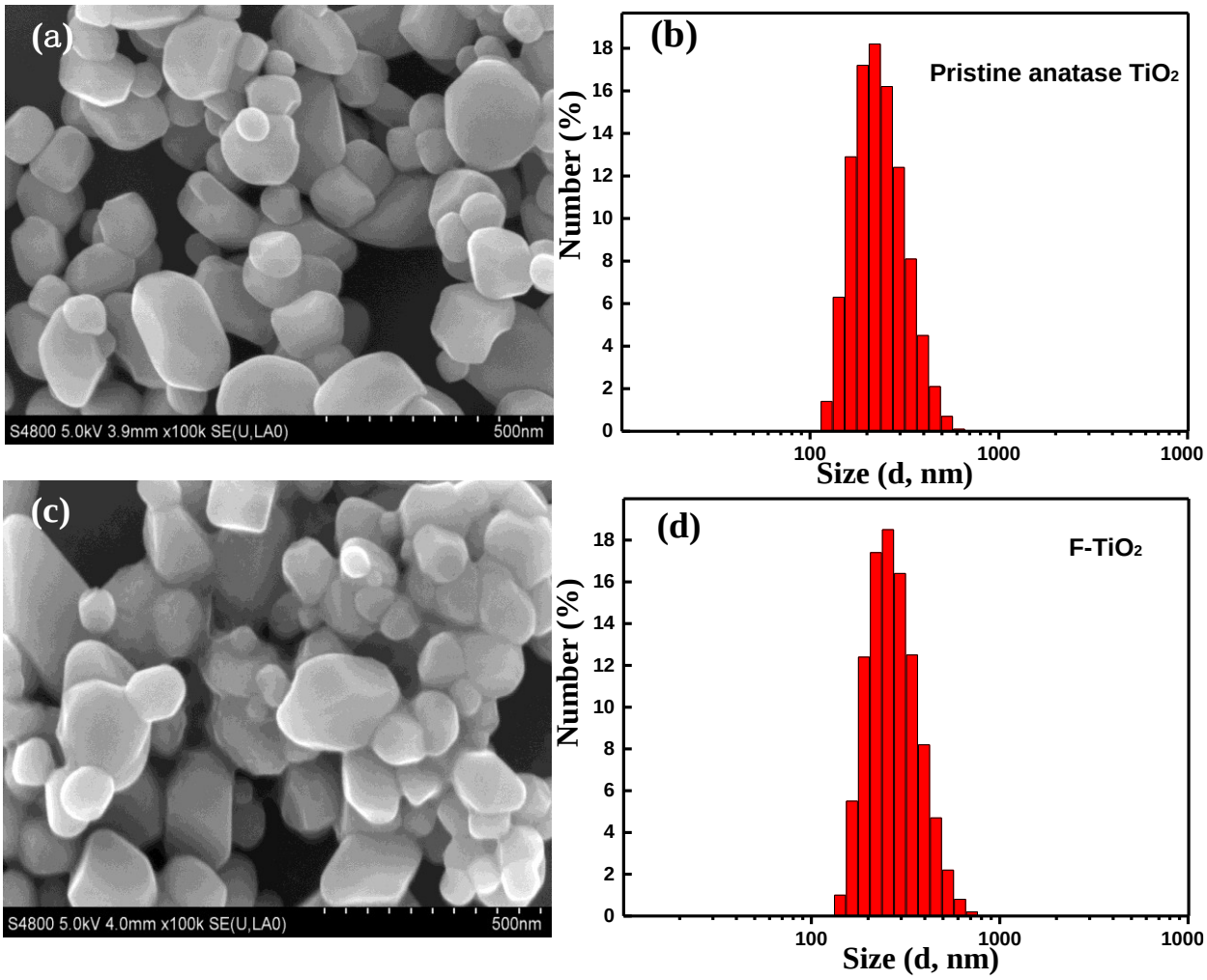

Figure 2

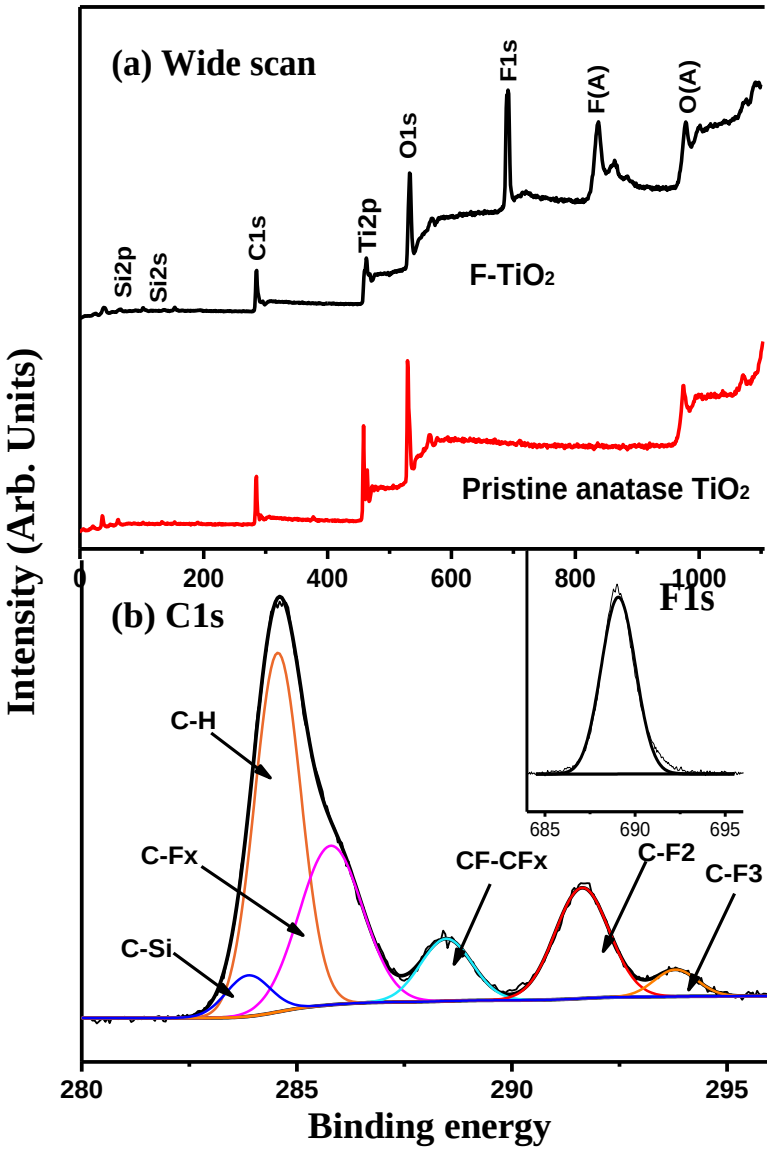

Figure 3

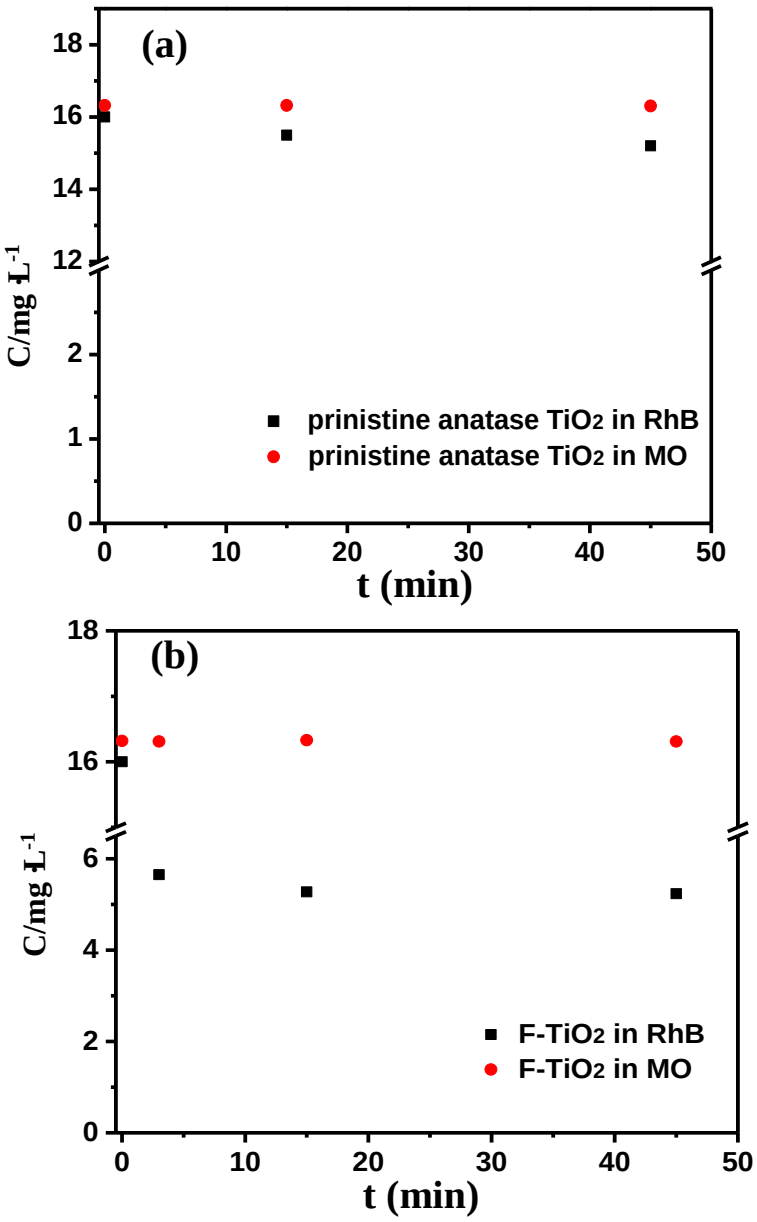

Figure 4

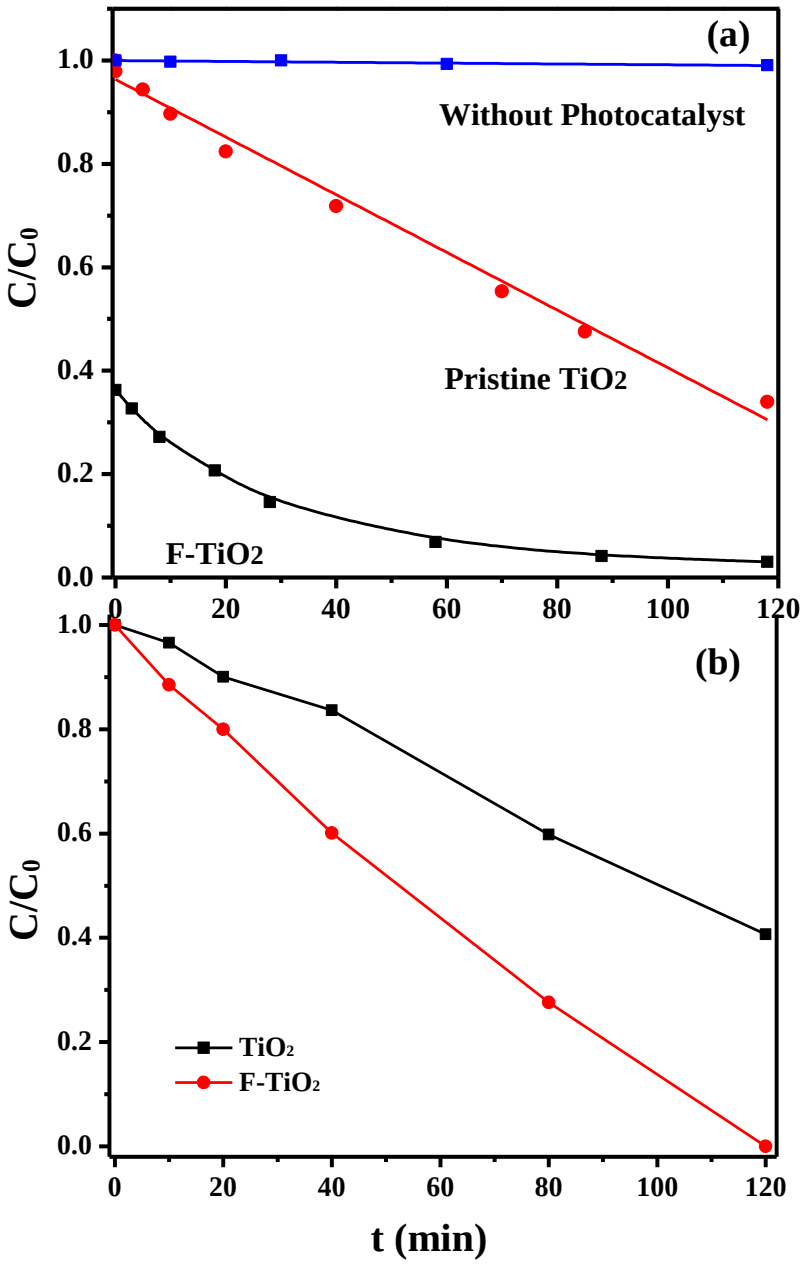

Figure 5

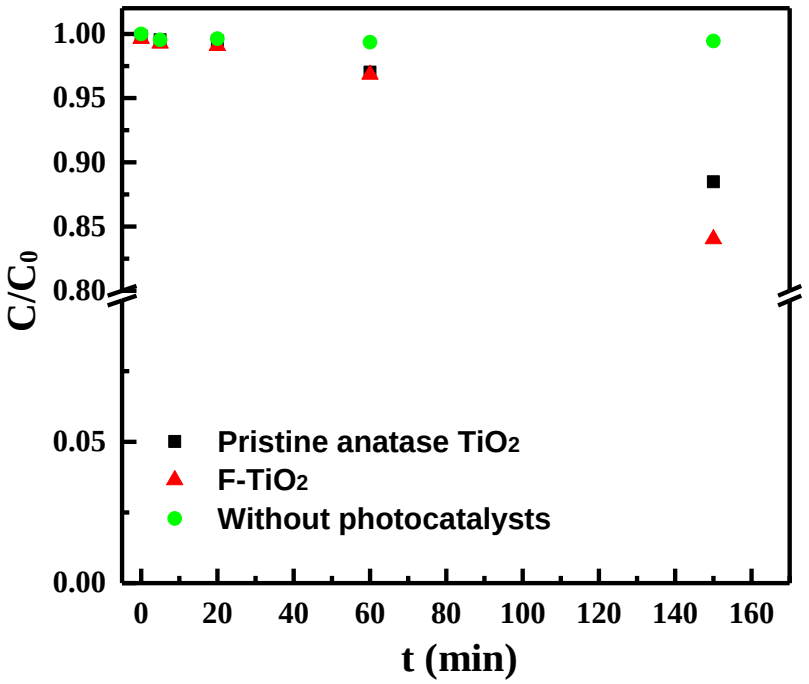

Figure 6

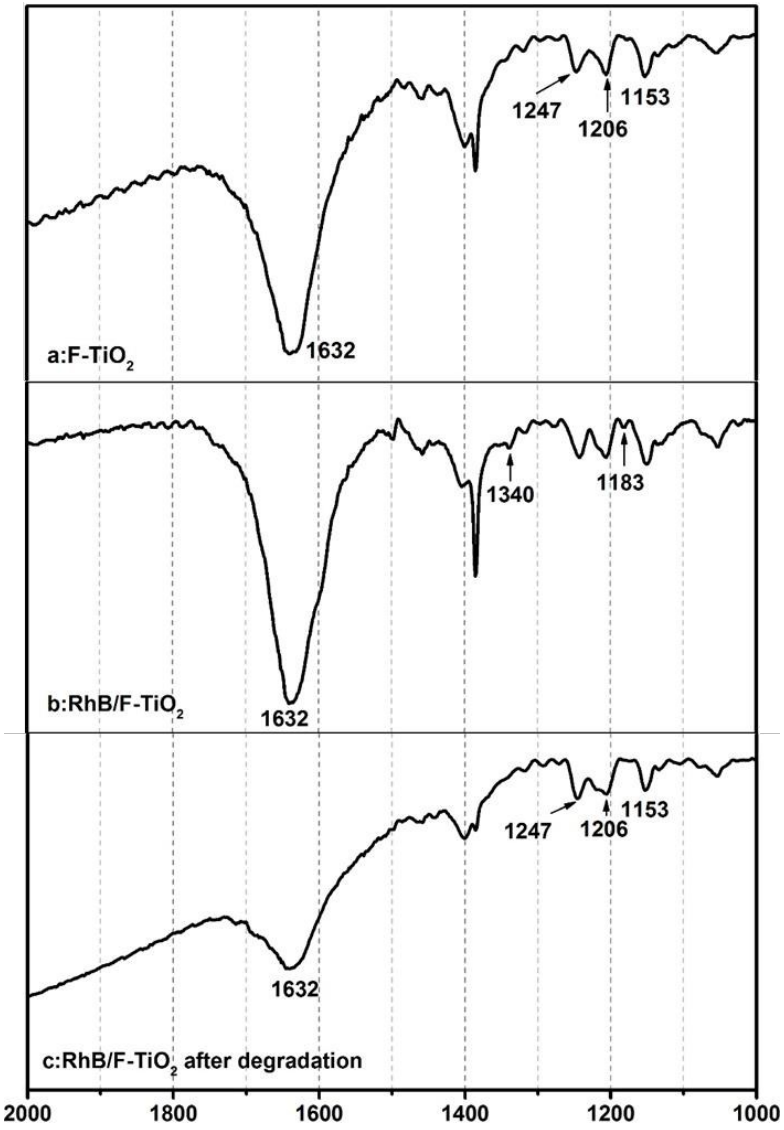

Figure 7

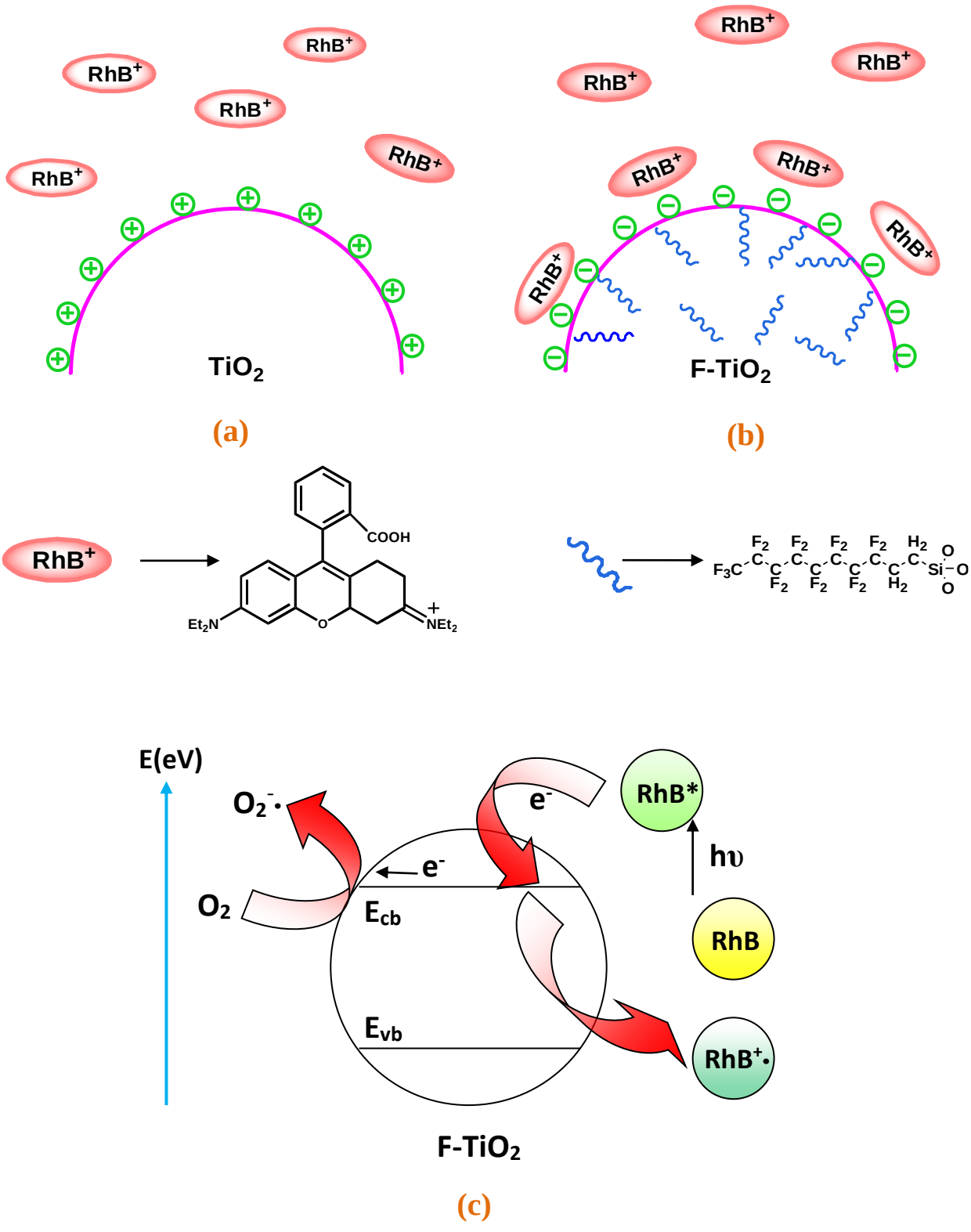

Figure 8

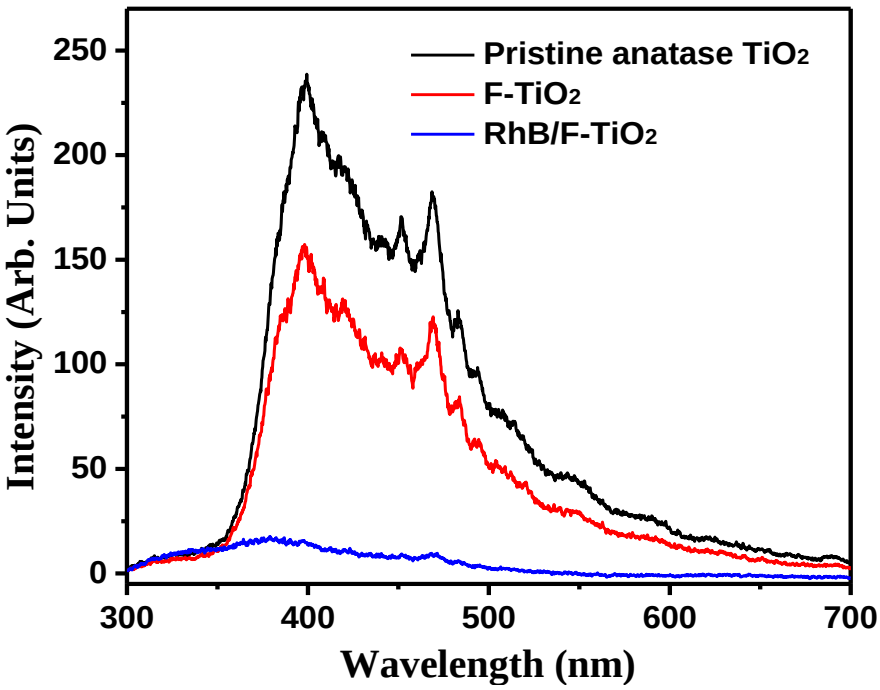

Figure 9

Graphic Abstract

Title: Adsorption and Photocatalytic Degradation Behaviors of Rhodamine Dyes on Surface-Fluorination TiO_2 under Visible Irradiation

Authors: Jing Guo, Shaojun Yuan, Wei Jiang, Hairong Yue, Zhe Cui, Bin Liang

Graphic Abstract

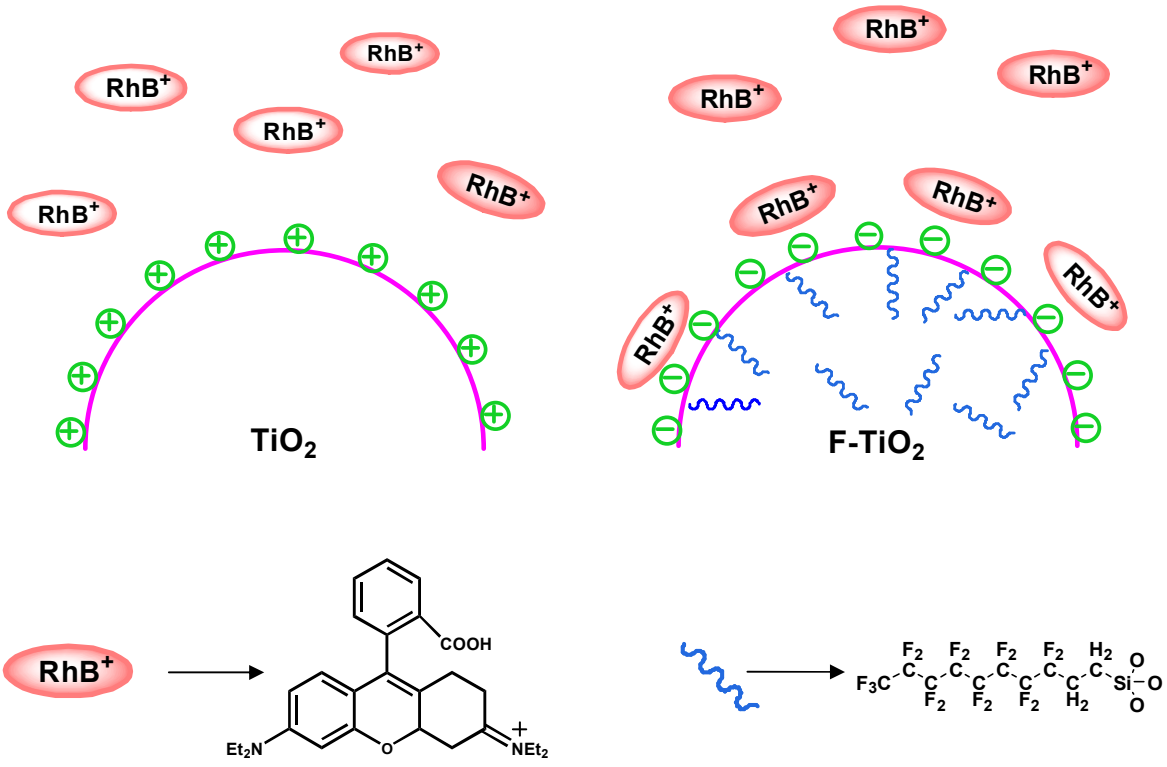

Adsorption and Photocatalytic Degradation Behaviors of Rhodamine Dyes on Surface-Fluorination TiO_2 under Visible Irradiation